Paper 128

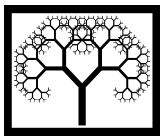

Proceedings of the Twelfth International Conference
on Computational Structures Technology,
B.H.V. Topping and P. Iványi, (Editors),
Civil-Comp Press, Stirlingshire, Scotland.

Uncertainty Analysis of the Dynamic Response of a Randomly Parametrized Corrugated Skin

A. Kundu[1], F.A. DiazDelaO[2], M.I. Friswell[1] and S. Adhikari[1]
[1]Civil and Computational Engineering Centre
Swansea University, Swansea, United Kingdom
[2]Institute for Risk and Uncertainty
University of Liverpool, Liverpool, United Kingdom

Abstract

Uncertainty analysis of computational models is essential to obtain a probabilistic description of the output quantities in the presence of uncertain model parameters or model inadequacy. Uncertainty quantification of the numerical model inputs, propagation of uncertainty to the model output and finally the analysis of response statistics, sensitivity, reliability, are all covered within the topic of uncertainty analysis. This has important applications in engineering design in terms of optimizing design variables under parameter fluctuations, obtaining confidence values associated with a novel design amongst others. However, the stochastic analysis of computational models are quite expensive. The objective of the work, described in this paper, is to develop a computational framework for efficient uncertainty analysis of structural dynamic systems. This has been applied to the design optimization of corrugated compliant skins in order to study its response sensitivity to its material properties and geometrical parameters. The sparse grid collocation technique has been utilized here as an efficient uncertainty propagation method for a multidimensional stochastic input. The sensitivity of the solution to the various sources of input uncertainty is studied using the Sobol's indices for sensitivity measure. Important physical insight into the behavior of the model for various uncertainties in geometrical and parametric properties is provided by this analysis.

Keywords: stochastic structural dynamics, stochastic sensitivity, sparse-grid collocation, corrugated skin.

1 Introduction

Shape morphing in context of aerospace applications is being investigated enthusiastically due to it's potential of offering aerodynamically adaptive, light weight, effi-

cient solutions for aircraft technology would suit a wide variety of mission profiles. The novel design features encompass a wide spectrum of innovative design of structural components which exhibit highly anisotropic behavior to suit the requirements of high compliance combined with high strength. The mathematical idealization of these structures for the purpose of simulating their behavior under different loading conditions often suffers from lack of proper understanding of the elastic behavior of these structures, incomplete knowledge about their geometric (both macro and micro scale) or elastic parameters, or even limited fidelity of the model itself. As a result, it is essential to perform uncertainty analysis on the predicted behavior of these structures.

The passive methods of designing structures for optimum geometry, topology and material properties for morphing applications focus on developing novel microstructures for multifunctional composites, constructing variable stiffness laminates or designing anisotropic compliant skins amongst many. Some examples include, auxetic honeycombs [1] giving high Young's modulus and damping loss, curvilinear fibre laminates [2], elastomer-fibre-composite surface supported with flexible honeycomb structures [3], cellular honeycomb core composites [4]. The various passive morphing technologies employed in aerospace applications have been aptly reviewed in [5].

In the present work, we look into the design of corrugated skins which are potential candidates for aircraft morphing applications [6]. These are highly anisotropic skins which gives low modulus along the direction of corrugation and high strength in the direction orthogonal to it. Numerical and experimental studies with corrugated skins [7] and the deformation characteristics of the morphing wings with corrugated composites and skins have been studied in the literature [8, 9]. However, due to the intricate design of the corrugated skins, the parametric and geometrical properties of the skins required in the mathematical models can not be known for certain [10]. Often these uncertainties are irreducible due to the cost associated with their precise measurement. The present work aims to quantify these uncertainties with a probabilistic description and propagate these uncertainties to the dynamic system response of the corrugated skins. Thus, the countable set of random variables used to model the input uncertainty would form the stochastic input space of the mathematical model. Propagating this input randomness of the physical system to the response quantities (such as displacement, pressure, velocity) can be tackled with various uncertainty propagation techniques.

2 Stochastically parametrized corrugated skins

We assume a baseline model of the corrugated skin which corresponds to the deterministic model. A probabilistic description is incorporated into the various elastic (such as the bending stiffness, volume density) and the definitions of the geometric parameters (such as the height, width, angles of corrugation, surface topology). The description is typically provided with a set of random variables which introduce random perturbations into the geometry and elastic properties of the skin. Figure 1(a) shows a sketch of the side view of a unit cell with the corresponding geometry. Figure 1(b) shows the

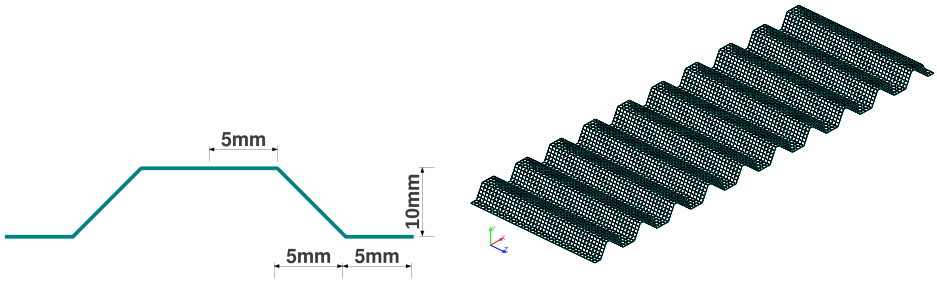

(a) Sketch of one corrugated unit (b) Meshed corrugated panel

Figure 1: Model of the corrugated panel employed in the analysis. (a) Unit cell; (b) Finite element model of the corrugated panel. The dimensions are: 300 mm in length, 75 mm in width, and 10 mm in height.

meshed geometry of the corrugated skin that has been employed in the analysis. This highly compliant skin is particularly important in morphing applications as discussed in Section 1.

Once the input geometric and/or the (elastic) parametric uncertainty has been propagated to the system response, it would be essential to have a quantitative measure of the sensitivity of the solution to the various input uncertainty. This helps to identify the parameters which are most sensitive to the response statistics. This is accomplished with a sensitivity analysis which is carried out using the concept of Sobol indices [11] which gives a quantitative estimate of the sensitivity of the solution to each source of uncertainty for a large input stochastic dimension. Thus it is possible to make an informed decision about which uncertainties can be ignored safely and the threshold values of the input variability for an uncertainty to become significant.

2.1 Description of input uncertainty

Consider a damped corrugated skin whose baseline model is given in Figure 1. Such corrugated skins are prone to geometric uncertainties (due to manufacturing) and material uncertainties, such as a random bending stiffness. A deterministic model of this composite corrugated skin has been studied previously [12].

A random field $a(\mathbf{r}, \theta) : \mathscr{D} \times \Theta$ over a spatial domain $\mathscr{D} \in \mathbb{R}^d$, may be expressed in a series expandable form following a spectral decomposition of the associated covariance kernel with the random field as

$$\int_{\mathscr{D}} C_a(\mathbf{r}_1, \mathbf{r}_2)\varphi_j(\mathbf{r}_1)\mathrm{d}\mathbf{r}_1 = \nu_j\varphi_j(\mathbf{r}_2), \quad \forall\ j = 1, 2, \cdots \tag{1}$$

The above is a homogeneous Fredholm integral equation of the second kind. If $\mathscr{C}_a\varphi$ is defined as $(\mathscr{C}_a\varphi)(\mathbf{r}_2) = \int_{\mathscr{D}} C_a(\mathbf{r}_1, \mathbf{r}_2)\varphi(\mathbf{r}_1)d\mathbf{r}_1, \quad \mathbf{r}_1, \mathbf{r}_2 \in \mathbb{R}^d$, it can be verified that $\mathscr{C}_a : L^2(\mathbb{R}^d) \to L^2(\mathbb{R}^d)$ is a linear operator on a vector space. Hence Equation 1 can be expressed as $\mathscr{C}_a\varphi = \nu\varphi$. A non-trivial solution to the above homogeneous

equation exists only for those values of ν which make $(I-\nu\mathscr{C}_a)$ singular, where I is the identity operator. The covariance functions C_a are usually bounded and symmetric, hence the associated linear operator $\mathscr{C}_a$ is compact and self-adjoint. The solution of the eigenvalue problem in Equation 1 yields ordered real eigenvalues $\nu = \{\nu_i : \nu_i \geq \nu_{i+1}\ \forall i$ and $\|C_a\|^2_{L^2\left(\mathbb{R}^d\times\mathbb{R}^d\right)} = \sum_i \nu_i^2\}$ and mutually orthogonal eigenfunctions $\varphi(\mathbf{r}_1)$ in $L^2(\mathbb{R}^d)$. Thus, from Mercer's theorem we can write

$$C_{a_M}(\mathbf{r}_1, \mathbf{r}_2) = \sum_{i=1}^{M} \nu_i \varphi(\mathbf{r}_1)\varphi(\mathbf{r}_2) \tag{2}$$

where C_{a_M} converges uniformly to C_a as $M \to \infty$.

The covariance function might also be a constructed at a discrete set of points on the physical domain. For example, the width or height of the corrugation between different corrugation units or the angles of corrugation ϕ_i within one corrugation unit and across various units. For these cases, the linear operator $\mathscr{C}_a$ would consist of a matrix of the covariance values at discrete set of chosen points. Thus the random field can be represented with a denumerable set of eigenvalues and eigenvectors of the covariance kernel using the Karhunen-Loève (KL) expansion as

$$a(\mathbf{r}, \theta) = a_0(\mathbf{r}) + \sum_{i=1}^{M} \sqrt{\nu_i}\widetilde{\xi}_i(\theta)\varphi_i(\mathbf{r}), \tag{3}$$

where $a_0(\mathbf{r}) = \mathrm{E}\left[a(\mathbf{r}, \theta)\right]$ is the mean, and $\widetilde{\xi}_i(\theta)$ are the mutually independent random variables with zero mean ($\mathrm{E}\left[\widetilde{\xi}_i\right] = 0$) and unit variance ($\mathrm{E}\left[\widetilde{\xi}_i^2\right] = 1$) for $i = 1, \ldots, M$. The above expansion is valid for Gaussian random fields. General non-Gaussian random fields are expressed in a mean-square convergent series using the Wiener-Askey chaos expansion scheme [13, 14], where the basis functions are constructed with a denumerable set (M) of independent random variables $\boldsymbol{\xi} = [\xi_1, \xi_2, \ldots, \xi_M]^\intercal \in \Theta^{(M)}$ where $\Theta^{(M)} \subset \Theta$. These basis functions span the stochastic Hilbert space and hence the problem can be equivalently formulated on a finite dimensional probability space $\left(\Theta^{(M)}, \mathscr{F}^{(M)}, P^{(M)}\right)$ where $\Theta^{(M)} = \mathrm{Range}(\boldsymbol{\xi})$, $\mathscr{F}^{(M)}$ is the associated Borel σ-algebra and $P^{(M)}$ is a probability measure. The formulation presented in this paper is applicable to this kind of general decomposition of the random field.

2.2 Stochastic dynamical system

A randomly parametrized structural dynamic system is defined on the domain $\mathscr{D} \subset \mathbb{R}^d$ ($d \leq 3$), subject to an externally applied deterministic excitation f_0. The equilibrium condition gives the following stochastic partial differential equation (SPDE)

$$\rho\frac{\partial^2 u}{\partial t^2} + \mathfrak{L}_\eta\frac{\partial u}{\partial t} + \mathrm{div}(\sigma_a(u)) = f_0 \quad \text{ on } \mathscr{D},\ \ t \in \mathbb{R}^+ \tag{4}$$

with the associated Dirichlet boundary condition

$$u = 0 \quad \text{on } \partial\mathscr{D}.$$

where $\sigma_a(u)$ is the stress related to the displacement field u, ρ is the mass density, and t is the time. $\mathfrak{L}_\eta$ denotes the damping operator, with η as the damping parameter, and can be used to represent different damping models such as strain rate dependent viscous damping or velocity dependent viscous damping. $(\Theta, \mathscr{F}, P)$ is a probability space where $\theta \in \Theta$ is a sample point from the sampling space Θ, $\mathscr{F}$ is the associated Borel σ-algebra and P is a probability measure. The constitutive equations relating the stress field to the displacement u is given as

$$\sigma_a(u) = a(\mathbf{r}, \theta) : \varepsilon(u)$$

where a is the Hooke's elasticity tensor and is a second order, stationary, square integrable random field such that $a : \mathbb{R}^d \times \Theta \to \mathbb{R}$. Here ':' denotes the standard tensor inner product of second order tensors. Depending on the physical problem, the random field $a(\mathbf{r}, \theta)$ can be used to model different physical systems.

For the harmonic analysis of the system Equation 4 is written in the frequency domain (using Fourier transformation) as

$$-\omega^2 \rho \widetilde{u} + i\omega \left(\mathfrak{L}_\eta \widetilde{u}\right) + \text{div}\left(\sigma_a(\widetilde{u})\right) = \widetilde{f}_0(\omega) \qquad \omega \in \Omega, \tag{5}$$

where Ω denotes the frequency space of the problem. Here $\widetilde{f}_0(\omega)$ and $\widetilde{u}(\omega)$ are the frequency dependent complex amplitudes of the harmonic input excitation and the system response respectively.

The FE treatment of the governing SPDE involves spatial discretization of the physical domain $\mathscr{D} \in \mathbb{R}^d$ into elemental domains $\mathscr{D}^h$ (h is the mesh parameter size). The Doob-Dynkin lemma ensures that the solution of the SPDE can be expressed in terms of the finite dimensional input vector $\boldsymbol{\xi}(\theta)$ (as in Equation 3). Thus the solution of the discretized FE system is sought in the tensor product Hilbert space $\mathscr{H}(\mathscr{D}^h \times \Theta)$. This space can be expressed in a separable form with the Hilbert spaces $\mathscr{H}_1$ and $\mathscr{H}_2$ such that $\mathscr{H} \simeq \mathscr{H}_1 \otimes \mathscr{H}_2$. The system matrices inherit the randomness of the input stochastic parameters and hence the stochastic linear system for structural dynamics takes the form

$$\begin{aligned} \left[-\omega^2 \mathbf{M}(\theta) + j\omega \mathbf{C}(\theta) + \mathbf{K}(\theta)\right] \widetilde{\mathbf{u}}(\omega, \theta) &= \widetilde{\mathbf{f}}_0(\omega) \\ \text{or,} \quad \left(\mathbf{A}_0(\omega) + \sum_{i=1}^{M} \xi_i(\theta) \mathbf{A}_i(\omega)\right) \widetilde{\mathbf{u}}(\omega, \theta) &= \widetilde{\mathbf{f}}_0(\omega) \end{aligned} \tag{6}$$

where $\mathbf{M}(\theta)$, $\mathbf{C}(\theta)$ and $\mathbf{K}(\theta)$ are the random mass, damping and stiffness matrices respectively, which have been combined to obtain the complex frequency dependent coefficient matrices $\mathbf{A}_i(\omega),\ i = 0, 1, \ldots, M$. Also, when the random variables are expanded in the series expansion form of Equation 3

$$\mathbf{M}(\theta) = \mathbf{M}_0 + \sum_{i=1}^{p_1} \mu_i(\theta) \mathbf{M}_i \in \mathbb{R}^{n \times n} \quad \text{and} \quad \mathbf{K}(\theta) = \mathbf{K}_0 + \sum_{i=1}^{p_2} \nu_i(\theta) \mathbf{K}_i \in \mathbb{R}^{n \times n} \tag{7}$$

Here ($\mathbf{M}_0$ and $\mathbf{K}_0$) are the deterministic mass and stiffness matrices while ($\mathbf{M}_i$ and $\mathbf{K}_i$) are the corresponding perturbation components obtained from discretizing the mass and stiffness parameters with finite number of random variables ($\mu_i(\theta)$ and $\nu_i(\theta)$).

For such random system matrices, the natural frequencies of the system are also stochastic quantities which are functions of the input random variables. If we denote by $\boldsymbol{\phi}_k(\theta) \in \mathbb{R}^n, \ \ \forall \theta \in \Theta^{(M)}$ the eigenvectors of the system,

$$\mathbf{K}(\theta)\boldsymbol{\phi}_k(\theta) = \lambda_k(\theta)\mathbf{M}(\theta)\boldsymbol{\phi}_k(\theta); \quad k = 1, 2, \ldots n \tag{8}$$

Now for each sample realization, the system matrices $\mathbf{K}(\theta)$ and $\mathbf{M}(\theta)$ are symmetric and generally non-negative definite, the eigenpairs $[\lambda_k(\theta), \boldsymbol{\phi}_k(\theta)]$ can be expressed as a function of the input random variables $\boldsymbol{\xi}(\theta)$.

Again, the matrices of the eigenvalues and eigenvectors of the above generalized stochastic eigen-value problem are denoted by $\boldsymbol{\lambda}(\theta) = [\lambda_1(\theta), \lambda_2(\theta), \ldots, \lambda_n(\theta)]$ and $\boldsymbol{\Phi}(\theta) = [\boldsymbol{\phi}_1(\theta), \boldsymbol{\phi}_2(\theta), \ldots, \boldsymbol{\phi}_n(\theta)]$. Now, for each sample, the eigenvalues are ordered in the ascending order so that $\lambda_1(\theta) < \lambda_2(\theta) < \ldots < \lambda_n(\theta)$ for every $\theta \in \Theta^{(M)}$ with orthogonal eigenvectors $\boldsymbol{\Phi}$ which gives $\boldsymbol{\Phi}^T(\theta)\mathbf{K}(\theta)\boldsymbol{\Phi}(\theta) = \boldsymbol{\lambda}(\theta)$. The evaluation of the eigenvalues as a stochastic function of the input random variables is also a computationally expensive exercise and obtaining a stochastic functional representation of the quantities can be quite expensive. Hence in the following section, we look at the uncertainty propagation methods suitable to obtain a stochastic interpolant of these random quantities in the multidimensional stochastic space.

2.3 Uncertainty propagation scheme

Various uncertainty propagation techniques for a wide variety of stochastic structural dynamic systems exist in the literature which range from non-intrusive statistical simulation methods (such as the crude Monte Carlo simulation (MCS) and its variants [15]) to non-statistical analytical methods (such as the perturbation methods [16], the Neumann expansion method [17], hybrid metamodeling schemes [18] or Galerkin-based finite order chaos expansion methods [19]). Alternatively, there are sparse-grid stochastic collocation methods which rely on constructing the random solution using polynomial interpolation functions with a set of random responses evaluated at the zeros of these multidimensional stochastic interpolation functions [20]. This requires resolution of the random system response at the sparse grid collocation points. For high-dimensional stochastic problems, adaptive sparse-grid collocation techniques have been proposed which aims to represent the problem with few lower order terms [21, 22]. The computational evidence indicates the effectiveness of the sparse grid stochastic collocation method compared to full tensor and Monte Carlo approaches.

If a function $\mathbf{u}$ is expressed in the multivariate stochastic space $\theta \in \Theta^{(M)}$ of dimension M as $\mathbf{u} = \mathbf{u}^{i_1} \otimes \ldots \otimes \mathbf{u}^{i_M}$ where each of $\mathbf{u}^{i_j}$ denotes the function approximated along the j-th stochastic dimension, then the function $\mathbf{u}$ can be reconstructed in the M-dimensional stochastic space with polynomial basis functions of the random variables

as

$$\mathbf{u}^{i_1} \otimes \ldots \otimes \mathbf{u}^{i_M} = \sum_{j_1=1}^{m_{i_1}} \ldots \sum_{j_M=1}^{m_{i_M}} f(x_{j1=1}^{i_1}, \ldots, x_{jM=1}^{i_M}) \cdot \left(a_{j_1}^{i_1} \otimes \ldots \otimes a_{j_M}^{i_M}\right) \tag{9}$$

$$\text{where} \quad \mathbf{u}^{i_k}(f) = \sum_{j=1}^{n_i} f(x_j^{i_k}) \cdot a_j^{i_k}$$

is the approximation along each stochastic dimension. The above tensor product formula requires evaluation of the stochastic function at $(m_{i_1} \ldots m_{i_M})$ grid points. For very high dimensional problems, i.e. large M, the above method becomes computationally intensive and a sparse grid technique is implemented using Smolyak's algorithm as [23]

$$\mathscr{A}(q, M) = \sum_{q-M+1 \leq |\mathbf{i}| \leq q} (-1)^{q-|\mathbf{i}|} \cdot \binom{M-1}{q-|\mathbf{i}|} \cdot \mathbf{u}^{i_1} \otimes \ldots \otimes \mathbf{u}^{i_M} \tag{10}$$

where $\mathscr{A}(q, M)$ are linear combinations of product formulas given in Equation 9, $q \geq M$ and $\mathbf{i} = (i_1, \ldots, i_M)$ with $|\mathbf{i}| = i_1 + \ldots + i_M$ which requires fewer realizations of the stochastic response in order to obtain the complete response statistics. Hence to compute $\mathscr{A}(q, M)$ the response has to be evaluated at the sparse grid points

$$\mathscr{X}(q, M) = \bigcup_{q-M+1 \leq |\mathbf{i}| \leq q} \left(X^{i_1} \times \ldots \times X^{i_M}\right) \tag{11}$$

with $X^{i_k} = \left\{x_1^{i_k}, \ldots, x_{m_i}^{i_k}\right\}$ denoting the set of points used by $\mathbf{u}^{i_k}$. Here we have used the Smolyak formulas that are based on polynomial interpolation at the extrema of the Chebyshev polynomials. This gives a nested set of nodes which can be used to approximate the stochastic quantity.

Once the hierarchal basis function has been constructed, the sample solutions at various sets of points in the stochastic space can be obtained using the approximation given in Equation 9. The stochastic system response or the eigenvalues of the structural dynamic system can be approximated using this approach to obtain an efficient functional representation of these quantities. It might be noted here that the sparse-grid stochastic collocation method is a non-intrusive technique which can be trivially parallelized, hence the solution is quite efficient for low to moderate stochastic dimensions.

3 Results & Discussions

The dynamic response of the randomly parametrized corrugated skin is being studied here. The uncertainties in the material and geometric properties which have been described probabilistically. This random fields have been expressed with a set of finite

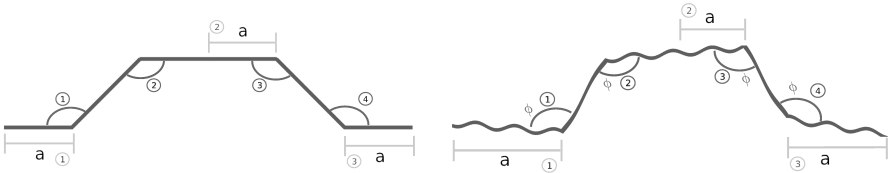

(a) Baseline corrugated unit (b) Perturbed corrugated unit

Figure 2: Perturbation of a corrugated unit for arbitrary randomness of the various geometrical parameters and random surface topology.

number of independent random variables. These random variables constitute the input stochastic space.

Each corrugation unit of the skin given in Figure 1 is defined by its width, height and the angle of corrugation. However, it is impossible to have an exact replication of the prescribed geometrical parameters given in the mathematical model. The aim here is to account for this uncertainty in the corrugation geometry and investigate its effect on the response and the equivalent stiffness of the corrugated skin. Additionally there might be random surface roughness present in the corrugated skin which can be quantified with the correlation of the position coordinates as a function of the distance between two points.

The random parameters of the corrugated skin are utilized to model the various sources of input uncertainty and they are modeled as follows.

- The topology of the corrugated skins is assumed to be a random field which is described with an exponential covariance function

$$C_r(\mathbf{r}_1, \mathbf{r}_2) = \exp\left\{-\frac{\|\mathbf{r}_1 - \mathbf{r}_2\|_{L^2}}{L_c}\right\}$$

  The random field has been approximated with 10 uniform random variables which models the perturbation of the (x, y) coordinates of the skin.

- The 11-th random variable models the thickness of the corrugated panel as a uniform random variable.

- The 12-th random variable models the Young's modulus as a uniform random variable.

The input standard deviation σ chosen for each of these random parameters has been chosen to be equal for all cases, $\sigma = 0.5$. Hence we have a total of 3 random inputs (topology, thickness and elastic constant) where the random field model with 10 independent uniform random variables is chosen to describe the random topology of the corrugated skin and 1 uniform random variable is used to model the thickness and 1 to model the elastic constant.

The stochastic solution of this system has been obtained with the stochastic collocation method where the finite element solver has been employed to obtain the solution

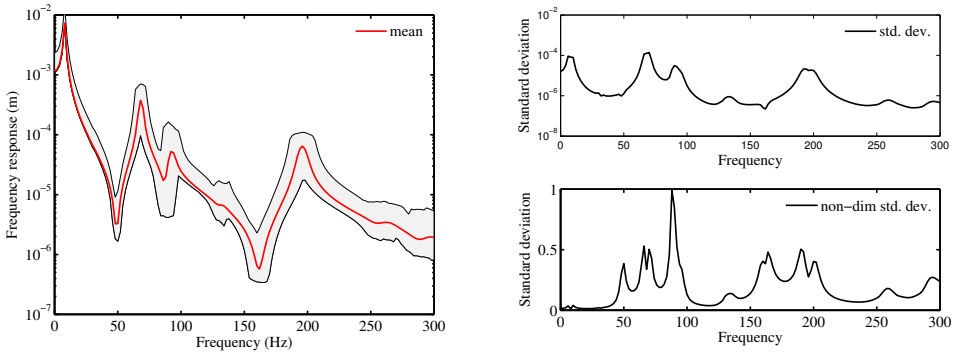

(a) Mean of the response (b) Standard deviation of the response

Figure 3: (a) Mean frequency response function in the ensemble of the various reponse functions obtained for each sample realization of the random geometrical configuration of the corrugated skin. The sample realizations FRF have been obtained with a sparse grid collocation technique using Chebyshev interpolation functions. The system has been parametrized with 12 iid random variables. (b) Standard deviation of the response and the corresponding non-dimensional standard deviation obtained by normalization with the mean response.

at a set of points in the stochastic space. It is known that the propagation of multiplicative input uncertainty to the system response leads to the stochastic solutions which can be expressed as polynomials of random variables. The accuracy of finite order polynomial interpolation of course depends on the smoothness of the function. Under the assumptions of moderately smooth response functions, we have used the Chebyshev interpolation functions to approximate the response. This is based on polynomial interpolation of the objective function in the stochastic space and hence produces good approximations of the solution. Additionally, this scheme has the benefit of nesting of nodes which has substantial computational advantage. The sparse grid method produced a solution of accuracy $\approx 10^{-3}$ with as few as $9,000$ sample points.

Figure 4 shows the plots of the eigenvalues of the random corrugated skin along with their PDF. Figure 4(a) shows the statistical range of the first six eigenvalues along with their upper and lower bounds. The bounds have been calculated as (Mean $\pm 3\times$ Standard Deviation). Figure 4(b) shows the PDF of the first 6 eigenvalues of the random structural dynamic system. The overlap in the PDFs of the eigenvalues, especially for the $3-6$ eigenvalues, signifies that the natural frequency values can cross each other for different samples.

Figure 5 shows the probability density functions (PDFs) and the joint PDFs of the first 6 eigenvalues of the randomly parametrized system. The diagonal plots in the grid of figures in Figure 5 shows the PDFs of the eigenvalues from 1 to 6 (1st row to last row respectively). The figures in the lower triangle shows the joint PDFs between pairs of eigenvalues. The plots show a high degree of correlation between the eigenvalues

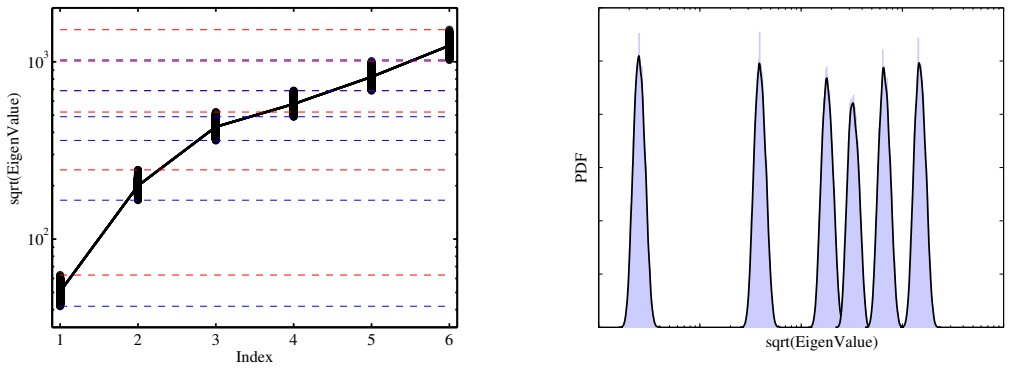

(a) Bounds of the first 6 eigenvalues

(b) PDFs of the first 6 eigenvalues

Figure 4: The first 6 eigenvalues of the stochastically parametrized dynamic system and their upper and lower bounds ($\pm 3 \times \sigma$) (b) Probability density functions of the first 6 eigen values of the stochastically parametrized dynamical system and their overlaps. The input uncertainty is represented with 12 iid random variables representing various geometrical and elastic parameters.

of the system. While this is expected since the eigen functions depend on the same set of input random variable, yet dependence may not always imply correlation. For e.g., the 4th random variable is found to exhibit a lesser degree of correlation with the other eigenvalues. Hence, in general, a small change in any one eigenvalues due to an input variability would result in modification of all the eigenvalues.

Figure 6 shows the scatter plot of the square root of the first 6 eigenvalues (which are the natural frequencies of the system in rad/s) with respect to the various random variables ξ_i modeling the input uncertainty. Here we have shown the variability with respect to the two dominant random variables ξ_1 and ξ_2 modeling the random geometry while the ξ_{11} models the random thickness and ξ_{12} corresponds to the random Young's modulus. The scatter plots provide a qualitative estimate of the sensitivity patterns of the eigenvalues to the various input randomness. The specific shape of the sample clouds in Figures 6(a) and 6(d) highlight the sensitivity of the eigenvalues to first and the twelfth random variables.

However, it is essential to obtain a quantitative estimate of the sensitivity values of the random variables to the input random variables to have a clear idea of the impact of the random inputs to the stochastic response quantities. This is discussed in the following section.

3.1 Sobol's sensitivity measure

A quantitative estimate of the sensitivity of the model output to the various input random variables can be provided by the Sobol indices [11]. We assume that the random samples $\boldsymbol{\xi}(\theta) \in \Theta^{(M)}$ where $\Theta^{(M)}$ is the M-dimensional stochastic space and $\boldsymbol{\xi} = \{\xi_1, \ldots, \xi_M\}$ is the vector of random variables. If the response quantity

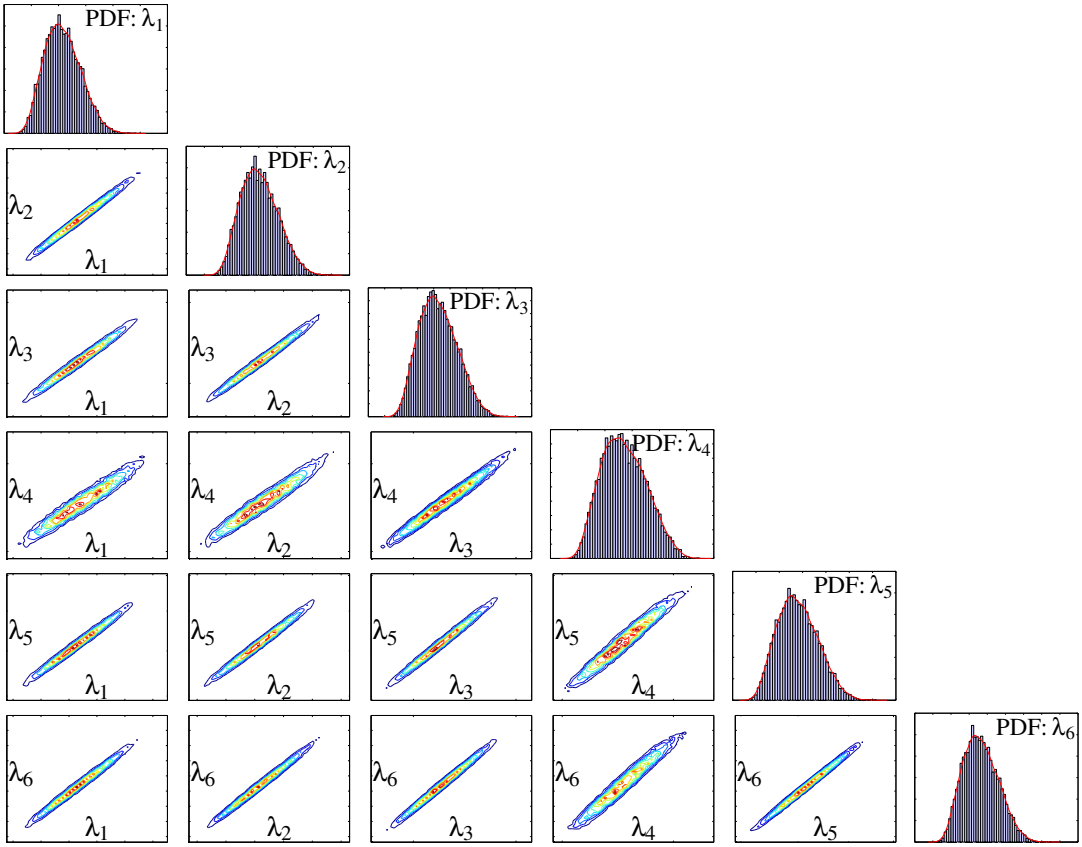

Figure 5: Probability densities and joint probability densities of the first 6 eigenvalues of the stochastically parametrized dynamical system. The figures on the diagonal gives the PDFs of the eigenvalues with 1st eigenvalue on the first row till the 6th on the last row while the figures in the lower triangle gives the joint PDF of a pair of eigenvalues.

$\mathbf{u} = \mathbf{u}(\boldsymbol{\xi}(\theta))$ expressed as a function of the input uncertainty is expanded as

$$\mathbf{u}(\boldsymbol{\xi}) = \mathbf{u}_0 + \sum_{i=1}^{M} \mathbf{u}_i(\xi) + \sum_{1 \le i < j \le M} \mathbf{u}_{ij}(\xi_i, \xi_j) + \ldots + \mathbf{u}_{1,2,\ldots,M}(\xi_1, \ldots, \xi_M) \qquad (12)$$

then it is seen that the expansion terms successively gives the dependence of the stochastic functions on the individual random variables followed by their interaction terms. The term $\mathbf{u}_0$ is the mean value of the function while the summands are orthogonal to each other in the sense

$$\int_{\Theta^M} \mathbf{u}_{i \in \mathscr{I}} \mathbf{u}_{j \in \mathscr{I}} d\boldsymbol{\xi} = 0 \quad \text{for} \quad \{i_1, \ldots, i_k\} \neq \{j_1, \ldots, j_k\} \qquad (13)$$

where i, j are elements of the cardinality $\mathscr{I}$. The successive terms of the expansion maybe derived analytically and is unique when the functions $\mathbf{u}(\boldsymbol{\xi}\theta)$ is square-integrable in $\Theta^{(M)}$. When the input random variables are independent of each other

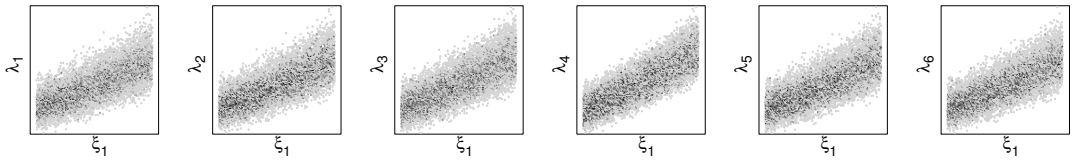

(a) Scatter plot of the first 6 eigenvalues with ξ_1

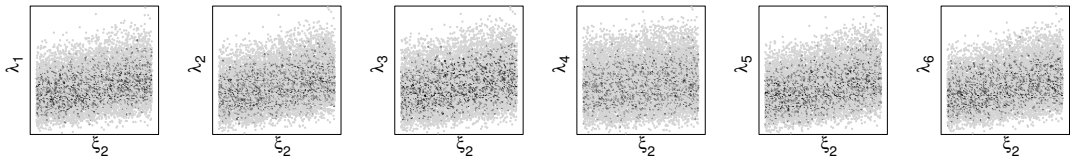

(b) Scatter plot of the first 6 eigenvalues with ξ_2

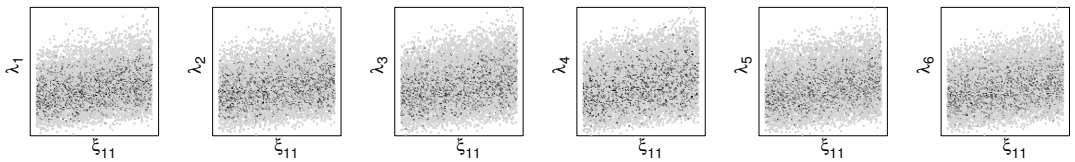

(c) Scatter plot of the first 6 eigenvalues with ξ_{11}

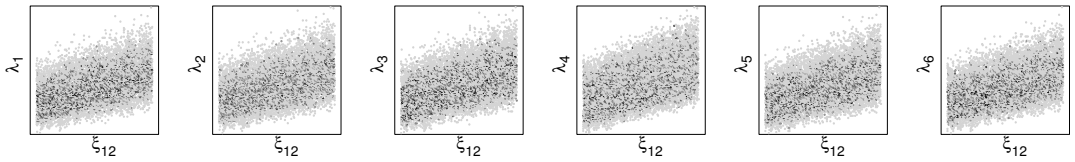

(d) Scatter plot of the first 6 eigenvalues with ξ_{12}

Figure 6: Scatter plot of the first 6 eigenvalues of the randomly parametrized dynamical system with random variables 1 and 2 (models geometric uncertainty), 11 (thickness), 12 (Young's modulus) for the same value of input standard deviation, $\sigma = 0.5$ for all sources of uncertainty.

the total variance of $\mathbf{u}(\boldsymbol{\xi}(\theta))$ i.e. $D = \mathrm{Var}\left[\mathbf{u}(\boldsymbol{\xi}(\theta))\right]$ can be written as

$$D = \sum_{i=1}^{M} D_i + \sum_{1 \le i < j \le M} D_{ij} + \ldots + D_{1,\ldots,M} \tag{14}$$

$$\text{where} \quad \int_{\Theta^{(M)}} \mathbf{u}_{i_1,\ldots,i_s}(x_{i_1},\ldots,x_{i_s}) dx_{i_1},\ldots,dx_{i_s}$$

where $D_{i_1,\ldots,i_k}$ are the *partial variances* in the expression. The expression for partial variances follows from Equations 12–13. The Sobol indices are defined as

$$\mathcal{S}_{i_1,\ldots,i_k} = \frac{D_{i_1,\ldots,i_k}}{D} \tag{15}$$

along with the expression

$$\mathcal{S} = \sum_{i=1}^{M} \mathcal{S}_i + \sum_{1 \le i < j \le M} \mathcal{S}_{ij} + \ldots + \mathcal{S}_{1,\ldots,M} = 1 \tag{16}$$

The relative importance of the individual input random variables in the response quantities are provided by the values of the Sobol indices. The first order Sobol index associated with the i-th random variable is given by $\mathcal{S}_i = D_i/D$ which can also be written as

$$\mathcal{S}_i(\mathbf{u}(\boldsymbol{\xi})) = \frac{\mathrm{Var}\left[\mathrm{E}\left[\mathbf{u}(\boldsymbol{\xi})|\xi_i\right]\right]}{\mathrm{Var}\left[\mathbf{u}(\boldsymbol{\xi})\right]}\,, \qquad i = 1, \ldots, M \tag{17}$$

While the Sobol indices can be calculated analytically from a finite order chaos expansion [24] or from a set of sample solutions using either Monte Carlo based approaches or other sample based schemes usually employed for uncertainty propagation.

In the present study, the samples response have been calculated by interpolating the stochastic system response with the sparse grid collocation method using the Chebyshev interpolation functions. Once the stochastic interpolant has been constructed, the sample realizations can be generated very efficiently by providing the sample points in the multi-dimensional stochastic space.

R.V.	λ_1	λ_2	λ_3	λ_4	λ_5	λ_6
ξ_1	0.552858	0.572822	0.605915	0.675468	0.592541	0.592996
ξ_2	**0.069691**	**0.081345**	0.053878	0.010606	**0.082869**	**0.081395**
ξ_3	0.039061	0.029039	0.035367	0.012760	0.026999	0.030290
ξ_4	0.036874	0.007629	0.010088	0.003642	0.017856	0.014268
ξ_5	0.015467	0.009411	0.003374	0.005202	0.006109	0.005624
ξ_6	0.011263	0.018786	0.001356	0.001576	0.002831	0.005073
ξ_7	0.007001	0.008647	0.005209	0.000709	0.001962	0.003482
ξ_8	0.003541	0.004256	0.007036	0.000899	0.000089	0.000884
ξ_9	0.004508	0.004831	0.004929	0.002948	0.002616	0.001010
ξ_{10}	0.002345	0.002523	0.002295	0.000917	0.007127	0.000180
ξ_{11}	0.051539	0.051970	**0.054579**	**0.056574**	0.052424	0.052920
ξ_{12}	0.203692	0.206073	0.216003	0.228251	0.206734	0.208912

Table 1: Sobol's sensitivity indices for the first six eigenvalues of the randomly parametrized stochastic system. The first order Sobol indices are shown. The colors are used to highlight the four largest sensitivity values in the descending order as: red, blue, **black**, magenta.

We show in Table 1 the sensitivity of the first six eigenvalues $\{\lambda_j,\ j = 1, \ldots, 6\}$ to the 12 random variables $\{\xi_i,\ i = 1, \ldots, 12\}$. The largest values are highlighted in red and it is seen that the all the first six eigenvalues are most sensitive to ξ_1 which is the first random variable associated with the highest KL mode of the random field expansion. The second most sensitive source of variability for the eigenvalues is the

Random Variable	Frequency 10Hz		Frequency 40Hz	
	1st order	Total order	1st order	Total order
ξ_1	0.596887	0.681848	0.602800	0.603187
ξ_2	**0.075407**	**0.116021**	0.123432	0.145555
ξ_3	0.043067	0.042681	0.057587	0.058535
ξ_4	0.039702	0.072457	0.016432	0.016592
ξ_5	0.012125	0.017601	0.007975	0.009162
ξ_6	0.011535	0.019496	0.014371	0.017048
ξ_7	0.010525	0.011409	0.017610	0.021410
ξ_8	0.003221	0.007876	0.014139	0.013327
ξ_9	0.006270	0.013490	0.006598	0.005191
ξ_{10}	0.001792	0.004069	0.004362	0.004849
ξ_{11}	0.051548	0.069512	0.044449	0.052172
ξ_{12}	0.094710	0.140751	**0.082410**	**0.093695**

Table 2: Sobol's sensitivity indices for the frequency response function at two different frequency values (10 Hz and 40 Hz). The first order and the total order Sobol indices are shown. The colors are used to highlight the four largest sensitivity values in the descending order as: red, blue, **black**, magenta.

random Young's modulus (modeled with ξ_{12}). Following this, the stochastic sensitivity of the various eigenvalues are different.

The first order and the total order Sobol indices have been evaluated and presented in Table 2 which shows the sensitivity values of the frequency response at 10Hz and 40Hz. The response is most sensitive to the first random variable (ξ_1) modeling the random geometry, while the next most sensitive random input is different for the various stochastic quantities. It is also seen that the sensitivity ranking in terms of the first order values can be different from that of the total order values, as is the case with the values marked in magenta (4th most important) for the frequency response at 10 Hz. However this is not often the case since the high order interaction terms in the calculation of the total order Sobol indices are often quite less compared to the first order terms. It might be mentioned that the credible interval of the predicted sensitivity values have been contained to below 15% for the five most dominant uncertainties. This denotes an acceptable accuracy for the evaluated sensitivity values.

4 Summary & Future Work

The uncertainty analysis and the stochastic sensitivity analysis of the corrugated skin studied here is particularly important in terms of obtaining the statistical behaviour of the dynamical system model subject to input uncertainties and quantifying the sensitivity of the response quantities to the different uncertainty sources. The present model has been analysed with respect to various geometric and elastic variability in the model input. The random topology of the corrugated skin is described with a random field

model with a covariance function giving the spatial correlation of the random field. A sparse grid stochastic collocation technique with a nested Chebyshev grid has been used to propagate the input uncertainty to the response quantities. The influence of the input uncertainty on the response statistics has been analyzed with first order Sobol indices which gives the dominant components of the random variables modeling the input uncertainty. The collocation scheme performs quite efficiently in terms of predicting the statistical summary of the stochastic response quantities. The analysis provides a quantitative estimate of the influence of the various input uncertainties on the stochastic response of the random structural dynamic system.

It would be interesting to look at the following aspects of uncertainty analysis of the corrugated skins in future work in this domain

- Investigation into the optimal design of the corrugated skins for maximizing the performance objectives of these compliant skins with inputs from the stochastic sensitivity analysis.
- Incorporate model calibration within the stochastic framework which can update the model with experimental data within a Bayesian framework.
- Stochastic uncertainty propagation into equivalent low-fidelity models which can provide a computationally solution scheme.

It has to be mentioned that it is important to have an equivalent low-fidelity model of the corrugated skin which in its final form would be parametrized and used in the conceptual design of a morphing aircraft wing. Thus, we need to parametrize the response of this stochastic corrugated skin in terms of a set of equivalent elastic parameters. The propagation of input uncertainty to these equivalent parameters is a complicated exercise and would be tackled with various uncertainty propagation methods in a computationally efficient solution scheme. The impact of geometrical uncertainties in the estimation of equivalent parameters would be an important area of study.

Acknowledgments

AK and MIF acknowledge funding from the European Research Council through Grant No. 247045 entitled “Optimisation of Multi-scale Structures with Applications to Morphing Aircraft”. SA acknowledges the financial support from The Royal Society of London through the Wolfson Research Merit Award.

References

[1] G.J. Murray, F. Gandhi, “Auxetic honeycombs with lossy polymeric infills for high damping structural materials”, in *21st International Conference on Adaptive Structures and Technologies 2010, ICAST 2010*, pages 96–105, 2010.

[2] M.A. Nik, K. Fayazbakhsh, D. Pasini, L. Lessard, "Surrogate-based multi-objective optimization of a composite laminate with curvilinear fibers", *Composite Structures*, 94(8): 2306–2313, 2012.

[3] E.A. Bubert, B.K.S. Woods, K. Lee, C.S. Kothera, N.M. Wereley, "Design and fabrication of a passive 1D morphing aircraft skin", *Journal of Intelligent Material Systems and Structures*, 21(17): 1699–1717, 2010.

[4] K.R. Olympio, F. Gandhi, "Flexible skins for morphing aircraft using cellular honeycomb cores", *Journal of Intelligent Material Systems and Structures*, 21 (17): 1719–1735, 2010.

[5] H. Baier, L. Datashvili, "Active and morphing aerospace structures-a synthesis between advanced materials, structures and mechanisms", *International Journal of Aeronautical and Space Sciences*, 12(3): 225–240, 2011.

[6] C. Thill, J. Etches, I. Bond, K. Potter, P. Weaver, "Morphing skins", *Aeronautical Journal*, 112(1129): 117–139, 2008.

[7] P. Ghabezi, M. Golzar, "Mechanical Analysis of Trapezoidal Corrugated Composite Skins", *Applied Composite Materials*, pages 1–13, 2012.

[8] R. Ge, B. Wang, C. Mou, Y. Zhou, "Deformation characteristics of corrugated composites for morphing wings", *Frontiers of Mechanical Engineering in China*, 5(1): 73–78, 2010.

[9] C. Thill, J.D. Downsborough, S.J. Lai, I.P. Bond, D.P. Jones, "Aerodynamic study of corrugated skins for morphing wing applications", *Aeronautical Journal*, 114(1154): 237–244, 2010.

[10] A. Kundu, F. DiazDelaO, S. Adhikari, M. Friswell, "A hybrid spectral and metamodeling approach for the stochastic finite element analysis of structural dynamic systems", *Computer Methods in Applied Mechanics and Engineering*, 270(0): 201 – 219, 2014.

[11] A. Saltelli, P. Annoni, I. Azzini, F. Campolongo, M. Ratto, S. Tarantola, "Variance based sensitivity analysis of model output. Design and estimator for the total sensitivity index", *Computer Physics Communications*, 181(2): 259 – 270, 2010.

[12] I. Dayyani, S. Ziaei-Rad, H. Salehi, "Numerical and Experimental Investigations on Mechanical Behavior of Composite Corrugated Core", *Applied Composite Materials*, 19: 705–721, 2012.

[13] D.B. Xiu, G.E. Karniadakis, "The Wiener-Askey polynomial chaos for stochastic differential equations", *Siam Journal on Scientific Computing*, 24(2): 619–644, 2002.

[14] X.L. Wan, G.E. Karniadakis, "Beyond wiener-askey expansions: Handling arbitrary pdfs", *Journal of Scientific Computing*, 27((-3): 455–464, 2006.

[15] M. Papadrakakis, V. Papadopoulos, "Robust and efficient methods for stochastic finite element analysis using Monte Carlo simulation", *Computer Methods in Applied Mechanics and Engineering*, 134(3-4): 325–340, 1996.

[16] M. Kleiber, T.D. Hien, *The Stochastic Finite Element Method*, John Wiley, Chichester, 1992.

[17] W.Q. Zhu, Y.J. Ren, W.Q. Wu, "Stochastic FEM Based on Local Averages of

Random Vector Fields", *Journal of Engineering Mechanics*, 118(3): 496–511, 1992.

[18] A. Kundu, S. Adhikari, "Transient Response of Structural Dynamic Systems with Parametric Uncertainty", *Journal of Engineering Mechanics*, 140(2): 315–331, 2014.

[19] R. Ghanem, P.D. Spanos, *Stochastic Finite Elements: A Spectral Approach*, Springer-Verlag, New York, USA, 1991.

[20] I. Babuška, F. Nobile, R. Tempone, "A stochastic collocation method for elliptic partial differential equations with random input data", *SIAM Review*, 52(2): 317–355, 2010.

[21] X. Ma, N. Zabaras, "An adaptive high-dimensional stochastic model representation technique for the solution of stochastic partial differential equations", *Journal of Computational Physics*, 229(10): 3884–3915, 2010.

[22] J.D. Jakeman, S.G. Roberts, *Local and dimension adaptive stochastic collocation for uncertainty quantification*, Volume 88, 2013, pages 181–203.

[23] V. Barthelmann, E. Novak, K. Ritter, "High dimensional polynomial interpolation on sparse grids", *Advances in Computational Mathematics*, 12(4): 273–288, 2000.

[24] B. Sudret, "Global sensitivity analysis using polynomial chaos expansions", *Reliability Engineering and System Safety*, 93(7): 964–979, 2008.